

# Calculation of resistive magnetohydrodynamics and two-fluid tearing modes by example of reversed-field-pinch-like plasma

V. A. Svidzinski and H. Li

*Los Alamos National Laboratory, Los Alamos, New Mexico 87545, USA*

(Received 26 November 2007; accepted 7 April 2008; published online 15 May 2008)

An algorithm suitable for numerical solution of linear eigenmode problems in resistive magnetohydrodynamics (MHD) and two-fluid MHD models without prior approximations is presented. For these plasma models, sets of equations suitable for numerical solution are derived and the details of the algorithm of this solution are given. The algorithm is general and is suitable for solution of boundary (eigenmode) problems for different plasma configurations. It is most effective, however, in one-dimensional models since the grid size has to be sufficiently small in order to resolve the tearing layer together with the scale of the size of the plasma. The technique is applied for solving for tearing eigenmodes in reversed field pinch (RFP) -like plasma in plane geometry. Results of resistive MHD and two-fluid models are compared in this case, showing that the two-fluid effects on tearing modes in RFPs are sizable. © 2008 American Institute of Physics.

[DOI: [10.1063/1.2917916](https://doi.org/10.1063/1.2917916)]

## I. INTRODUCTION

Tearing instabilities play an important role in laboratory plasmas and in space and astrophysical applications; see, e.g., Ref. 1. They are thought to be responsible for fast reconnection of magnetic fields, relaxation to the Taylor state, and the dynamo effect in reversed field pinch (RFP).<sup>2-6</sup> The most common models used to study tearing instabilities are single fluid resistive magnetohydrodynamics (MHD)<sup>7,8</sup> and two-fluid MHD.<sup>9-13</sup> While the resistive MHD model is justified for some plasma parameters, the less restrictive two-fluid model is generally more suitable for studying the tearing modes. In particular, two-fluid theory predicts faster growth of the instability, which is closer to the observations. The two-fluid model becomes inaccurate when kinetic effects become important, in particular when the size of the ion gyroradius is comparable with the width of the tearing layer. In this case, kinetic theory should be used.

Since resistive MHD and two-fluid models are important tools in studying tearing instabilities, one has to be able to effectively solve the formulated problems within these plasma models. Equations governing tearing instability are complicated, especially in the two-fluid model. As a result, respective studies inevitably involve a number of simplifying assumptions and restrictions such as assuming that ions are immobile (electron MHD), use strong guide field approximation, or consider limiting cases of either cold or hot plasmas. Also a standard assumption is that the tearing layer width is much smaller than the size of the system, which allows separate solutions within the tearing layer and in the outer region. This assumption is not always accurate, in particular in highly resistive laboratory plasma.

For an effective study of tearing instabilities in different plasmas, it is important to have a practical way of finding the tearing modes for a specified plasma equilibrium in the two models without making any prior assumptions or approximations. We present here a numerical algorithm that is suitable for solving the linear eigenmode problem in resistive MHD

and two-fluid models without any prior approximations. This algorithm is most effective in one-dimensional models since the grid size has to be sufficiently small in order to resolve the tearing layer on the scale of the size of the plasma. It can be generalized to models with higher spatial dimensions (with more efforts involved) with the limitations on the size of the tearing layer relative to the size of the plasma. The algorithm is general. In addition to resistive MHD and two-fluid models, it is effective for solving plasma wave problems for arbitrary frequency in the cold plasma approximation. Our approach is unlikely to be new; it is probably used by others in one way or another. We believe, however, that the details of the algorithm are the most important part for understanding how to solve such problems, and these details are often not included in publications. An alternative way to find a linear eigenmode is to evolve equations in time.<sup>14</sup> This approach is more limited. It is more numerically intensive, not effective near marginal stability, and is limited to the fastest growing mode. We formulate sets of equations that are appropriate for the solution of boundary problems in the two models and present the details on how to solve them. The same approach can be used by others in the field for solving similar problems or as a tool for verification of large computer codes.

The algorithm is formulated for the case of tearing eigenmodes in one-dimensional (1D) plasma in force-free equilibrium in plane geometry bounded by two conducting walls. Conversion to cylindrical or other 1D geometries is straightforward. We expect the algorithm to work equally well for cases of equilibria with nonuniform pressure profiles or with equilibrium plasma flows. As a particular application, we calculate linear tearing eigenmodes in plasma with RFP-like parameters. We consider unstable RFP-like force-free plasma equilibrium in plane geometry and calculate tearing eigenmodes in resistive MHD and two-fluid models. Results show that in the RFP case, two-fluid effects on tearing modes

are sizable. The same approach can be used in other applications.

Equations suitable for solution of the boundary problem by this algorithm in resistive MHD and two-fluid models are derived in Secs. II and III. The algorithm of numerical solution of these equations is presented in Sec. IV. Results of calculations in the two models for RFP plasma parameters are given in Sec. V. Examples of application of this approach to resistive MHD modes and plasma waves in cylindrical geometry are given in the Appendix.

## II. RESISTIVE MHD MODEL

Consider plasma in plane geometry occupying the region  $0 \leq x \leq 2a$ . Conducting walls are located at  $x=0$  and  $x=2a$ . Plasma is uniform in  $y$  and  $z$  coordinates. We consider solutions of resistive MHD equations that are periodic in the  $y$  coordinate and do not depend on  $z$ . We use normalization

$$x = a\tilde{x}, \quad v = v_A\tilde{v}, \quad t = \tau_A\tilde{t},$$

$$B = B_0\tilde{B}, \quad E = B_0\frac{v_A}{c}\tilde{E}, \quad j = \frac{c}{4\pi a}\tilde{j},$$

$$\rho = \rho_0\tilde{\rho}, \quad p = p_0\tilde{p}, \quad \tau_A = \frac{a}{v_A},$$

$$\tau_R = \frac{4\pi a^2}{c^2\eta_0}, \quad S = \frac{\tau_R}{\tau_A}, \quad \beta_0 = \frac{8\pi p_0}{B_0^2},$$

where  $v_A$  is Alfvén speed,  $\tau_A$  and  $\tau_R$  are Alfvén and resistive time scales, and  $S$  is the Lundquist number.  $\rho_0$  and  $p_0$  are equilibrium plasma density and pressure. In the normalized variables, resistive MHD equations are<sup>2</sup>

$$\frac{\partial \rho}{\partial t} + \nabla \cdot (\rho \mathbf{v}) = 0, \quad (1)$$

$$\rho \left[ \frac{\partial \mathbf{v}}{\partial t} + (\mathbf{v} \cdot \nabla) \mathbf{v} \right] = -\frac{\beta_0}{2} \nabla p + (\nabla \times \mathbf{B}) \times \mathbf{B}, \quad (2)$$

$$\frac{\partial \mathbf{B}}{\partial t} = \nabla \times (\mathbf{v} \times \mathbf{B}) - \frac{1}{S} \nabla \times (\nabla \times \mathbf{B}), \quad (3)$$

$$\frac{\partial p}{\partial t} = -\gamma p \nabla \cdot \mathbf{v} - \mathbf{v} \cdot \nabla p, \quad (4)$$

where  $\gamma=5/3$  is an adiabatic factor. In the above equations, plasma resistivity is assumed to be uniform and the dissipative term containing the Lundquist number  $S$  is omitted in Eq. (4).

In this geometry, there are RFP-like force-free equilibria with uniform pressure and density profiles and zero plasma velocity. Such equilibrium magnetic field satisfies

$$\nabla \times \bar{\mathbf{B}} = \lambda \bar{\mathbf{B}}. \quad (5)$$

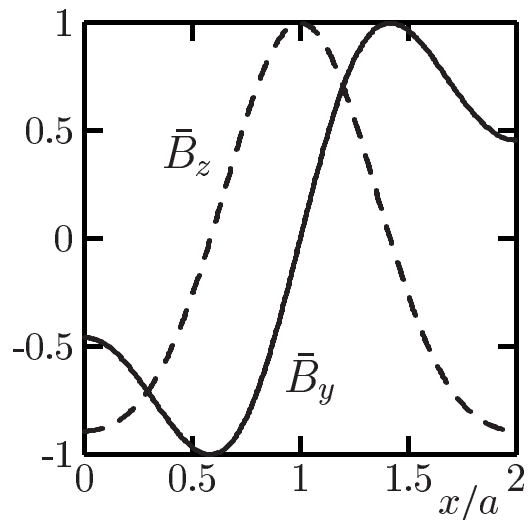


FIG. 1. Components of equilibrium magnetic field.  $\Theta_0=2$ ,  $\alpha_0=2$ .

We consider equilibrium  $\lambda$  profiles in the form

$$\lambda(x) = 2\Theta_0[1 - (x-1)^{\alpha_0}]. \quad (6)$$

Equation (5) leads to

$$\bar{B}_y = -\frac{1}{\lambda} \bar{B}_z' \bar{B}_z'' - \frac{\lambda'}{\lambda} \bar{B}_z' + \lambda^2 \bar{B}_z = 0.$$

These equations are solved numerically subject to the boundary conditions  $\bar{B}_y(1)=0$ ,  $\bar{B}_z(1)=1$ . Components of equilibrium magnetic field for  $\Theta_0=2$ ,  $\alpha_0=2$  are presented in Fig. 1. As in the case of cylindrical RFP equilibrium, the component  $\bar{B}_z$  reverses at some distance along the  $x$  axis. Normalized equilibrium field components in this geometry satisfy  $\bar{B}_y^2 + \bar{B}_z^2 = 1$ . Since  $\bar{B}_y$  crosses zero only at  $x/a=1$ , there is only one resonant surface for perturbations around this equilibrium, located at  $x/a=1$ .

Equations (1)–(4) are linearized about this equilibrium, and time and space dependence proportional to  $e^{-i\omega t +iky}$  is considered. Field components are converted to local coordinates connected with local direction of equilibrium magnetic field, such that  $B_x = B_x$ ,  $B_y = \beta B_\eta + \alpha B_\parallel$ ,  $B_z = -\alpha B_\eta + \beta B_\parallel$ , where  $\alpha = \bar{B}_y$ ,  $\beta = \bar{B}_z$ . The linearized equations in local coordinates are reduced to

$$\frac{k}{S} (ikB_x - \beta B_\eta' + \lambda \alpha B_\eta - \alpha B_\parallel' - \lambda \beta B_\parallel) + \omega B_x + \alpha k v_x = 0, \quad (7)$$

$$\frac{1}{S} [-B_\eta'' + (\lambda^2 + k^2) B_\eta - 2\lambda B_\parallel' - \lambda' B_\parallel] + \frac{k\alpha}{\omega} \frac{1}{\omega^2 - \frac{\beta_0 \gamma}{2} k^2}$$

$$\times \left[ -ik \left( \omega^2 - \frac{\beta_0 \gamma}{2} \alpha^2 k^2 \right) (-\alpha B_\eta + \beta B_\parallel) \right.$$

$$\left. + \lambda \left( \omega^2 - \frac{\beta_0 \gamma}{2} \alpha^2 k^2 \right) B_x - \frac{\beta_0 \gamma}{2} \omega \beta k v_x' \right]$$

$$+ \lambda v_x - i\omega B_\eta = 0, \quad (8)$$

$$\begin{aligned}
& \frac{1}{S}[-B''_{\parallel} + (\lambda^2 + k^2)B_{\parallel} + 2\lambda B'_{\eta} + \lambda' B_{\eta}] \\
& + \frac{k\beta}{\omega} \frac{1}{\omega^2 - \frac{\beta_0\gamma}{2}k^2} \left[ ik \left( \omega^2 - \frac{\beta_0\gamma}{2}\alpha^2 k^2 \right) (-\alpha B_{\eta} + \beta B_{\parallel}) \right. \\
& \left. - \lambda \left( \omega^2 - \frac{\beta_0\gamma}{2}\alpha^2 k^2 \right) B_x + \frac{\beta_0\gamma}{2} \omega \beta k v'_x \right] + v'_x - i\omega B_{\parallel} \\
& = 0, \tag{9}
\end{aligned}$$

$$\begin{aligned}
& \frac{\omega}{\omega^2 - \frac{\beta_0\gamma}{2}k^2} v''_x - \frac{k}{\omega^2 - \frac{\beta_0\gamma}{2}k^2} [(\beta\lambda)' B_x + ik(\alpha\beta B'_{\eta} \\
& - \lambda\alpha^2 B_{\eta} - \beta^2 B'_{\parallel} + \lambda\alpha\beta B_{\parallel})] + \frac{2\omega}{\beta_0\gamma} v_x \\
& + \frac{2i}{\beta_0\gamma} (B'_{\parallel} - ik\alpha B_x) = 0. \tag{10}
\end{aligned}$$

Primes in these equations denote derivative with respect to  $x$ . In the derivation, component  $B'_x$  is eliminated using  $\nabla \cdot \mathbf{B} = 0$ . Equation (7) is an algebraic equation for  $B_x$  and the others are second-order differential equations for  $B_{\eta}$ ,  $B_{\parallel}$ , and  $v_x$ , such that the overall order of Eqs. (7)–(10) is 6. One can derive a similar set of equations in which  $p$  is used in place of  $v_x$ . The equation for  $p$  in this case is also a second-order differential equation. We found, however, that our solution algorithm applied to such modified equations does not work. Thus it seems that the set of functions  $B_x$ ,  $B_{\eta}$ ,  $B_{\parallel}$ ,  $v_x$  is proper for numerical analysis while replacing  $v_x$  in this set by  $p$  results in a poorly defined problem.

The boundary value problem for the plasma eigenmodes is defined by Eqs. (7)–(10), and by the boundary conditions on the surface of the wall at  $x/a=0$  and  $x/a=2$ . Namely, at these locations  $E_{\eta}=0$ ,  $E_{\parallel}=0$ , and  $v_x=0$ . To find the eigenmode, we match solutions found in the regions  $0 \leq x/a \leq 1$  and  $1 \leq x/a \leq 2$  at the resonance point as follows. Applying three sets of boundary conditions at  $x/a=1$ ,  $B_{\eta}(1)=1$ ,  $B_{\parallel}(1)=0$ ,  $v_x(1)=0$ ;  $B_{\eta}(1)=0$ ,  $B_{\parallel}(1)=1$ ,  $v_x(1)=0$ ; and  $B_{\eta}(1)=0$ ,  $B_{\parallel}(1)=0$ ,  $v_x(1)=1$  for fixed  $\omega$ , we find the corresponding solutions of differential equations in these two regions, which are subject to the boundary conditions at  $x/a=0$  and  $x/a=2$ . These solutions are found numerically by a finite-difference method; the details of the algorithm used are given in Sec. IV.

The condition of continuity of  $B'_{\eta}$ ,  $B'_{\parallel}$ , and  $v'_x$  at  $x/a=1$  is then applied to an arbitrary linear combination of the three solutions. This leads to a set of three uniform algebraic equations for the unknown coefficients of the linear combination. Then we scan frequency  $\omega$  to find the eigenvalue for which these algebraic equations have a solution (the determinant of the corresponding matrix is equal to zero). For the found eigenvalue, relation between the coefficients provides the necessary relation between  $B_{\eta}$ ,  $B_{\parallel}$ , and  $v_x$  at  $x/a=1$  in the eigenmode. In the case of tearing modes, the eigenvalues  $\omega$  correspond to purely growing or decaying solutions such that the frequency scan along the imaginary axis is sufficient to

find the eigenvalue. In a more general case when roots have both real and imaginary parts, finding the solution requires more complicated approaches like integrating over closed contours to identify the root or using an iteration procedure to find the exact root when its location is approximately known.

One should note that matching solutions at the resonant surface look more suitable for numerical analysis than the use of other locations for this. Matching solutions outside the resonance layer result in a more stiff matrix for the eigenvalue analysis. Our calculations show, however, that while matching at resonant location results in a faster convergence of the determinant of the matching matrix, Eq. (34) in Sec. IV, with the increase of the number of grid points the overall efficiency of the eigenmode calculation does not degrade significantly when points outside of the resonance layer are used for the matching of solutions. Thus an arbitrary matching point can be used in the cases of multiple resonant surfaces or when there are no resonances in the plasma.

### III. TWO-FLUID MODEL

We consider the same geometry as in the case of the resistive MHD model. Plasma is uniform in  $y$  and  $z$  coordinates. Consider solutions of two-fluid MHD equations that are periodic in the  $y$  coordinate and do not depend on  $z$ . We use the same normalization as in the resistive MHD case except that parameter  $p_0$  now is the equilibrium pressure of a single species (electrons or ions) such that  $\beta_0 = 16\pi p_0 / B_0^2$ . Also new functions, particles densities  $n_e$ ,  $n_i$ , and temperatures  $T_e$ ,  $T_i$  are normalized by equilibrium values  $n_0$  and  $T_0$ , respectively.

Two-fluid equations, derived in Ref. 15, in normalized variables are

$$\frac{\partial n_e}{\partial t} + \nabla \cdot (n_e \mathbf{v}_e) = 0, \quad \frac{\partial n_i}{\partial t} + \nabla \cdot (n_i \mathbf{v}_i) = 0, \tag{11}$$

$$\begin{aligned}
\frac{\partial \mathbf{v}_e}{\partial t} + (\mathbf{v}_e \nabla) \mathbf{v}_e = & - \frac{\beta_0 m_i \nabla p_e}{4 m_e n_e} - \frac{m_i a}{m_e d_i} (\mathbf{E} + \mathbf{v}_e \times \mathbf{B}) \\
& - \frac{1}{S} \frac{m_i a^2}{m_e d_i^2} n_e (\mathbf{v}_e - \mathbf{v}_i), \tag{12}
\end{aligned}$$

$$\begin{aligned}
\frac{\partial \mathbf{v}_i}{\partial t} + (\mathbf{v}_i \nabla) \mathbf{v}_i = & - \frac{\beta_0 \nabla p_i}{4 n_i} + \frac{a}{d_i} (\mathbf{E} + \mathbf{v}_i \times \mathbf{B}) \\
& + \frac{1}{S} \frac{a^2 n_e^2}{d_i^2 n_i} (\mathbf{v}_e - \mathbf{v}_i), \tag{13}
\end{aligned}$$

$$p_e = n_e^\gamma, \quad p_i = n_i^\gamma, \tag{14}$$

where  $d_i = c / \omega_{pi}$  is the ion skin depth. In the above equations, viscous effects are ignored, the equation of state of each plasma component is adiabatic with  $\gamma=5/3$ , and the friction term in momentum equations is assumed to be isotropic. Electric and magnetic fields satisfy Maxwell's equations

$$\nabla \times \mathbf{E} = - \frac{\partial \mathbf{B}}{\partial t}, \tag{15}$$

$$\nabla \times \mathbf{B} = \mathbf{j} + \frac{v_A^2}{c^2} \frac{\partial \mathbf{E}}{\partial t}, \quad (16)$$

where  $\mathbf{j} = (a/d_i)(-n_e \mathbf{v}_e + n_i \mathbf{v}_i)$ .

We consider a force-free equilibrium with uniform pressure and density profiles and with equilibrium magnetic fields satisfying Eq. (5) and the  $\lambda$  profile defined by Eq. (6). We assume that the equilibrium current is carried by electrons while ions are stationary. Then the equilibrium electron velocity is  $\bar{\mathbf{v}}_e = -(\lambda d_i/a) \bar{\mathbf{B}}$ . This velocity satisfies  $(\bar{\mathbf{v}}_e \nabla) \bar{\mathbf{v}}_e = 0$ .

Equations (11)–(16) are linearized about this equilibrium, and time dependence proportional to  $e^{-i\omega t}$  is assumed. The set of linearized equations is

$$i\omega n_e = \nabla n_e \cdot \bar{\mathbf{v}}_e + \nabla \cdot \mathbf{v}_e, \quad i\omega n_i = \nabla \cdot \mathbf{v}_i, \quad (17)$$

$$i\omega \mathbf{v}_e = (\mathbf{v}_e \nabla) \bar{\mathbf{v}}_e + (\bar{\mathbf{v}}_e \nabla) \mathbf{v}_e + \frac{\beta_0 \gamma m_i}{4 m_e} \nabla n_e + \frac{m_i a}{m_e d_i} \times (\mathbf{E} + \bar{\mathbf{v}}_e \times \mathbf{B} + \mathbf{v}_e \times \bar{\mathbf{B}}) + \frac{1}{S} \frac{m_i a^2}{m_e d_i^2} (\mathbf{v}_e - \mathbf{v}_i), \quad (18)$$

$$i\omega \mathbf{v}_i = \frac{\beta_0 \gamma}{4} \nabla n_i - \frac{a}{d_i} (\mathbf{E} + \mathbf{v}_i \times \bar{\mathbf{B}}) - \frac{1}{S} \frac{a^2}{d_i^2} (\mathbf{v}_e - \mathbf{v}_i), \quad (19)$$

$$p_e = \gamma m_e, \quad p_i = \gamma m_i, \quad (20)$$

$$i\omega \mathbf{B} = \nabla \times \mathbf{E}, \quad (21)$$

$$\nabla \times \mathbf{B} = \mathbf{j} - i\omega \frac{v_A^2}{c^2} \mathbf{E}. \quad (22)$$

The linearized current is related to fluid velocities as  $\mathbf{j} = (a/d_i)(-n_e \bar{\mathbf{v}}_e - \mathbf{v}_e + \mathbf{v}_i)$ . In linearization of friction terms in Eqs. (12) and (13), we fixed electron and ion densities at their equilibrium values. This approximation is not mandatory; it is made here for simplification of initially approximate friction terms.

We assume that the  $y$  dependence of functions in these equations is proportional to  $e^{iky}$ . With this assumption, electron and ion densities can be found from Eq. (17) in terms of velocity components, which allows us to eliminate  $n_e$ ,  $n_i$  from other equations. The next step is to derive a set of equations suitable for numerical solution that is similar to Eqs. (7)–(10) used for numerical solution of the eigenvalue problem in the resistive MHD case. It appears, however, that such a derivation in the two-fluid case is a more complicated task. In the two-fluid case, the elimination of electric field from the equations results in the appearance of third derivatives of  $v_{ex}$  and  $v_{ix}$  with respect to  $x$  in the equations. The resulting set of equations is quite different from the one derived in the resistive MHD model and it seems that this set is not suitable for numerical solution. In order to find appropriate equations, one should instead eliminate magnetic field in the two-fluid case with the help of Eq. (21).

As in the case of resistive MHD, all vector components in the above equations are converted to local coordinates connected with local direction of equilibrium magnetic field. Eliminating  $n_e$ ,  $n_i$ , and  $\mathbf{B}$ , we find

$$E_x = \frac{i}{k^2 - \frac{v_A^2}{c^2} \omega^2} \left[ -k(\beta E'_\eta - \lambda \alpha E_\eta + \alpha E'_\parallel + \lambda \beta E_\parallel) + \omega \frac{a}{d_i} (v_{ix} - v_{ex}) \right], \quad (23)$$

$$ik\beta E'_x - E''_\eta + (\lambda^2 + \alpha^2 k^2) E_\eta - 2\lambda E'_\parallel - (\lambda' + \alpha \beta k^2) E_\parallel - i\omega \frac{a}{d_i} (v_{i\eta} - v_{e\eta}) - \frac{v_A^2}{c^2} \omega^2 E_\eta = 0, \quad (24)$$

$$ik\alpha E'_x + 2\lambda E'_\eta + (\lambda' - k^2 \alpha \beta) E_\eta - E''_\parallel + (\lambda^2 + k^2 \beta^2) E_\parallel - i\omega \frac{a}{d_i} (v_{i\parallel} - v_{e\parallel}) - \frac{\omega \lambda}{\omega + k\alpha \lambda \frac{d_i}{a}} \left[ v'_{ex} + ik(\beta v_{e\eta} + \alpha v_{e\parallel}) \right] - \frac{v_A^2}{c^2} \omega^2 E_\parallel = 0, \quad (25)$$

$$-i \frac{\beta_0 \gamma m_i}{4 m_e} \left\{ \frac{1}{\omega + k\alpha \lambda \frac{d_i}{a}} \left[ v''_{ex} + ik(\beta v'_{e\eta} + \alpha v'_{e\parallel} - \lambda \alpha v_{e\eta}) + \lambda \beta v_{e\parallel} \right] + \left[ \frac{1}{\omega + k\alpha \lambda \frac{d_i}{a}} \right]' \left[ v'_{ex} + ik(\beta v_{e\eta} + \alpha v_{e\parallel}) \right] \right\} + \frac{m_i a}{m_e d_i} \left[ E_x - \frac{i\lambda d_i}{\omega a} (\lambda E_\eta - E'_\parallel + ik\alpha E_x) + v_{e\eta} \right] - i\omega v_{ex} + \frac{1}{S} \frac{m_i a^2}{m_e d_i^2} (v_{ex} - v_{ix}) = 0, \quad (26)$$

$$-i \frac{\beta_0 \gamma}{4} \frac{1}{\omega} \left[ v''_{ix} + ik(\beta v'_{i\eta} + \alpha v'_{i\parallel} - \lambda \alpha v_{i\eta} + \lambda \beta v_{i\parallel}) \right] - \frac{a}{d_i} (E_x + v_{i\eta}) - i\omega v_{ix} - \frac{1}{S} \frac{a^2}{d_i^2} (v_{ex} - v_{ix}) = 0, \quad (27)$$

where the velocity components  $v_{e\eta}$ ,  $v_{e\parallel}$ ,  $v_{i\eta}$ , and  $v_{i\parallel}$  can be found from algebraic equations

$$\frac{\beta_0 \gamma m_i}{4 m_e} \frac{k\beta}{\omega + k\alpha \lambda \frac{d_i}{a}} \left[ v'_{ex} + ik(\beta v_{e\eta} + \alpha v_{e\parallel}) \right] + \frac{m_i a}{m_e d_i} \left[ E_\eta + \frac{\lambda k d_i}{\omega a} (\alpha E_\eta - \beta E_\parallel) - v_{ex} \right] - i\omega v_{e\eta} + \frac{1}{S} \frac{m_i a^2}{m_e d_i^2} (v_{e\eta} - v_{i\eta}) = 0, \quad (28)$$

$$\frac{\beta_0 \gamma m_i}{4 m_e} \frac{k\alpha}{\omega + k\alpha\lambda \frac{d_i}{a}} [v'_{ex} + ik(\beta v_{e\eta} + \alpha v_{e\parallel})] + \frac{m_i a}{m_e d_i} E_{\parallel} - i\omega v_{e\parallel} + \frac{1}{S} \frac{m_i a^2}{m_e d_i^2} (v_{e\parallel} - v_{i\parallel}) = 0, \quad (29)$$

$$\frac{\beta_0 \gamma k \beta}{4 \omega} [v'_{ix} + ik(\beta v_{i\eta} + \alpha v_{i\parallel})] - \frac{a}{d_i} (E_{\eta} - v_{ix}) - i\omega v_{i\eta} - \frac{1}{S} \frac{a^2}{d_i^2} (v_{e\eta} - v_{i\eta}) = 0, \quad (30)$$

$$\frac{\beta_0 \gamma k \alpha}{4 \omega} [v'_{ix} + ik(\beta v_{i\eta} + \alpha v_{i\parallel})] - \frac{a}{d_i} E_{\parallel} - i\omega v_{i\parallel} - \frac{1}{S} \frac{a^2}{d_i^2} (v_{e\parallel} - v_{i\parallel}) = 0. \quad (31)$$

In the above equations we neglected terms related to  $(\mathbf{v}_e \nabla) \mathbf{v}_e$  in Eq. (12). This assumption is not restrictive, it can be removed in general case.

When  $v_{e\eta}$ ,  $v_{e\parallel}$ ,  $v_{i\eta}$  and  $v_{i\parallel}$  are calculated from Eqs. (28)–(31) and substituted into Eqs. (24)–(27), the resulting set of equations for functions  $E_x$ ,  $E_{\eta}$ ,  $E_{\parallel}$ ,  $v_{ex}$  and  $v_{ix}$  becomes similar to the set of Eqs. (7)–(10) derived in the resistive MHD case with the difference that now electric field is in place of magnetic field and there are two separate equations with second derivatives of  $v_{ex}$  and  $v_{ix}$  instead of one equation including the second derivative of  $v$ . The resulting equations still contain  $E'_x$ , which should be eliminated in order for the equations to be suitable for numerical solution. In the case of resistive MHD,  $B'_x$ , used in place of  $E'_x$  here, was eliminated by using the equation  $\nabla \cdot \mathbf{B} = 0$ . Equation (23) cannot be used to eliminate  $E'_x$  from Eqs. (24) and (25) because these three equations are not independent.

It seems that the proper way to eliminate  $E'_x$  from Eqs. (24) and (25) is to get  $E'_x$  from the equation obtained by taking the divergence of Eq. (22). It is analogous to finding  $B'_x$  from the divergence of Eq. (21). One should note the importance of retaining the displacement current in Eq. (22) for this purpose. Thus, we find

$$E'_x = -ik(\beta E_{\eta} + \alpha E_{\parallel}) + \frac{a}{d_i} \frac{c^2}{v_A^2 i\omega} \times \left\{ -v'_{ex} + v'_{ix} + \frac{d_i}{a} \frac{k\alpha\lambda}{\omega + k\alpha\lambda \frac{d_i}{a}} [v'_{ex} + ik(\beta v_{e\eta} + \alpha v_{e\parallel})] + ik(-\beta v_{e\eta} - \alpha v_{e\parallel} + \beta v_{i\eta} + \alpha v_{i\parallel}) \right\}. \quad (32)$$

After the elimination of  $E'_x$  from Eqs. (24) and (25), the resulting set of equations contains one algebraic equation for  $E_x$ , Eq. (23), two equations with second derivatives of  $E_{\eta}$  and  $E_{\parallel}$ , and two equations with second derivatives of  $v_{ex}$  and  $v_{ix}$ . This set of equations is suitable for numerical analysis; it is similar to Eqs. (7)–(10).

For the numerical analysis, we do not derive explicitly the final rather bulky set of equations obtained by this procedure. Instead we manipulate the above equations numerically such that the obtained matrix formulation is equivalent to the matrix formulation corresponding to the final set of equations. The boundary conditions at  $x/a=0$  and 2 are  $E_{\eta}=0$ ,  $E_{\parallel}=0$ , and  $v_{ex}=0$ ,  $v_{ix}=0$ . The numerical algorithm for solution of the boundary value problem in this case is similar to the one used for solution of Eqs. (7)–(10) (it is described in Sec. IV) with the difference being that now there is an extra velocity component due to appearance of  $v_{ex}$  and  $v_{ix}$  in place of  $v_x$  and electric field components are used in place of the magnetic field components.

#### IV. ALGORITHM OF NUMERICAL SOLUTION OF THE BOUNDARY PROBLEM

To find the eigenmode, we match general solutions found in the regions  $0 \leq x/a \leq 1$  and  $1 \leq x/a \leq 2$  at the point  $x/a=1$  (as discussed in Sec. II, other matching points can also be used). The general solution in the first region is  $\mathbf{f}^1 = C_i \mathbf{f}^{1i}$ , where  $C_i$  are arbitrary constants and there is a summation over integer index  $i$ :  $i=1, 2, 3$  in the resistive MHD case and  $i=1, 2, 3, 4$  in the two-fluid model. Vector  $\mathbf{f}$  has components  $f_j = (B_{\eta}, B_{\parallel}, v_x)$  in the resistive MHD case and  $f_j = (E_{\eta}, E_{\parallel}, v_{ex}, v_{ix})$  in the two-fluid model. Functions  $\mathbf{f}^{1i}$  are the solutions of Eqs. (7)–(10) or the corresponding two-fluid equations with the boundary conditions at  $x/a=1$  as  $f_j^{1i} = \delta_{ij}$ , where  $\delta_{ij}=1$  if  $i=j$  and  $\delta_{ij}=0$  if  $i \neq j$ , and appropriate boundary conditions at  $x/a=0$ . In a similar way,  $\mathbf{f}^2 = C_i \mathbf{f}^{2i}$  is a general solution in the second region, with functions  $\mathbf{f}^{2i}$  satisfying boundary conditions at  $x/a=1$  as  $f_j^{2i} = \delta_{ij}$  and appropriate boundary conditions at  $x/a=2$ . The coefficients  $C_i$  are the same in the two regions in order for  $\mathbf{f}^1 = \mathbf{f}^2$  at the matching point.

The continuity of derivatives at  $x/a=1$  leads to a set of equations for unknown  $C_i$ ,

$$[(f_j^{1i})' - (f_j^{2i})'] C_i = 0. \quad (33)$$

The above equations are numbered by index  $j$  and there is a summation over index  $i$ . The derivatives are taken at  $x/a=1$ . Equations (33) have a solution when

$$\det[(f_j^{1i})' - (f_j^{2i})'] = 0. \quad (34)$$

Since functions  $f_j^{1i}$ ,  $f_j^{2i}$  depend on  $\omega$ , this condition defines the dispersion equation for the tearing modes (and for all other eigenmodes present in this geometry in these plasma models). When the condition of Eq. (34) is satisfied, the found relations between coefficients  $C_i$  define polarization of the fields in the eigenmode. The root of Eq. (34) is found by scanning  $\omega$  within some range or by iteration procedure when the initial value of  $\omega$  is close enough to the unknown root.

Functions  $\mathbf{f}^{1i}$  and  $\mathbf{f}^{2i}$  are found numerically. We present the details of the algorithm for calculating  $\mathbf{f}^{1i}$ ; functions  $\mathbf{f}^{2i}$  are calculated in a similar way. A number of equally spaced grid points is specified on the segment  $0 \leq x/a \leq 1$ . The

points are numbered by integers  $n=1, 2, \dots, N+1$  such that  $x_n/a=h(n-1)$ , where  $h=1/N$  is the distance between the adjacent points.  $n=1$  and  $n=N+1$  correspond to locations  $x/a=0$  and 1, respectively. The grid scale  $h$  should be small enough to resolve the scale of all solutions of the derived equations everywhere in the plasma. The derivatives at each grid point are approximated by differences,

$$f_j^n = \frac{f_j^{n+1} - f_j^{n-1}}{2h}, \quad f_j^{n'} = \frac{f_j^{n+1} - 2f_j^n + f_j^{n-1}}{h^2}. \quad (35)$$

The upper index  $i$  relating to boundary conditions at  $x/a=1$  is omitted in these equations. In the rest of this section, we use a convention that there is a summation over repeating lower indexes.

Applying formulas of Eq. (35) to plasma equations, one finds that field components  $f^n$  at a point  $x_n$  are related to field components at adjacent points,

$$A_{ij}^n f_j^n = R_{ij}^n f_j^{n+2l-3}. \quad (36)$$

Matrices  $A^n$  and  $R^n$  at each point  $x_n$  are defined by plasma equations. Indexes  $i$  and  $j$  numbering equations and field components have values  $i, j=1, 2, 3$  for resistive MHD equations and  $i, j=1, 2, 3, 4$  for two-fluid equations. Summation over integer index  $l=1, 2$  in the above equation defines the dependence on  $f^{n-1}$  and  $f^{n+1}$ . From Eq. (36), we find

$$f_i^n = A_{ij}^{1n} f_j^{n+2l-3}, \quad (37)$$

where

$$A_{ij}^{1n} = (A^n)^{-1}_{ik} R_{kl}^n.$$

The set of equations (37) for unknowns  $f_i^n$  is block tridiagonal. Its solution by Gaussian elimination (outlined in the next paragraph) is numerically stable when ordering either from the resonant layer or from the plasma boundary  $x/a=0$ .

We start from point  $n=N+1$  and move to the left to point  $n=1$  with the assumption that at every  $n$ ,

$$f_i^n = A_{ij}^{2n} f_j^{n-1} + A_i^{3n}, \quad (38)$$

where matrices  $A^2$  and  $A^3$  depend on  $n$ . Starting from  $n=N+1$  with  $A_{ij}^{2n}=0$  and  $A_i^{3n}=\delta_{ij}$  ( $j$  numbers boundary conditions at  $x/a=1$ , which are fixed here), Eqs. (37) and (38) define recurrent relations between matrices  $A^2$ ,  $A^3$  at points  $n$  and  $n+1$  as follows. If Eq. (38) is satisfied at a point  $n+1$ , then from Eq. (37) considered at point  $n$  and using Eq. (38) at point  $n+1$  we find

$$(\delta_{ij} - A_{i2k}^{1n} A_{kj}^{2n+1}) f_j^n = A_{i1j}^{1n} f_j^{n-1} + A_{i2j}^{1n} A_j^{3n+1}, \quad (39)$$

which defines

$$A_{ij}^{2n} = D_{ik}^{-1} A_{k1j}^{1n}, \quad A_i^{3n} = D_{ij}^{-1} A_{j2k}^{1n} A_k^{3n+1},$$

where

$$D_{ij} = \delta_{ij} - A_{i2k}^{1n} A_{kj}^{2n+1}.$$

Application of this recurrent procedure defines matrices  $A^2$  and  $A^3$  for  $n=N+1, N, \dots, 2$ . Boundary conditions at  $n=1$  define  $f_j^1$ . In the two-fluid case,  $f_j^1$  are specified directly. In the resistive MHD case, a combination of boundary conditions at  $x/a=0$  with Eq. (38) for  $n=2$  gives a solution for  $f_j^1$ .

When  $f_j^1$  are known,  $f_j^n$  are found for all  $n$  from subsequent application of Eqs. (38) for  $n=2, 3, \dots, N+1$ .

In the presented algorithm, the derived set of plasma equations is written in a form containing only field components corresponding to the ones that are specified in boundary conditions. The proper boundary conditions are a specification of either tangential components of electric field or tangential components of magnetic field plus a specification of normal components of velocities. This formulation ensures that during the above elimination procedure, the boundary problem with similar boundary conditions is formulated at each intermediate step. This reasoning formulates the algorithm for solution of boundary problems with local plasma response as follows. One should transform plasma equations to the form containing variables that correspond to the proper boundary conditions mentioned above (in general, tangential and normal field components are defined on coordinate surfaces obtained by continuous transformation of boundary surface) and then solve these equations by the described elimination procedure. This guidance can be used for formulation of the algorithm in other geometries and in problems with higher dimensions.

The presented algorithm is universal for solving electrodynamic problems with local linear dielectric response in different frequency ranges. Because of its implicit nature, it works equally well for lower-frequency MHD-type problems and for high-frequency waves in plasma. The presence of strongly growing or decaying solutions corresponding to small electron inertia (high plasma conductivity) or the presence of plasma resonances (Alfvén, cyclotron, lower, and upper hybrid resonances) does not impose restrictions in the solution by this algorithm (but still the grid size should be small enough to resolve these solutions). Two additional examples of application of this approach are given in the Appendix. One of them is a calculation of the eigenmodes in cylindrical geometry in the resistive MHD model for RFP equilibrium in a general case with current and pressure gradients at resonant surface. Another is a calculation of radio-frequency modes in cylindrical plasma in the model with plasma response defined by a cold plasma dielectric tensor. This example relates to wave modes in Helicon sources.

While the presented prescription is suitable in most general cases addressing the needs in solutions of corresponding boundary problems, it is not the only way to address such problems and in general it should not be assumed to be the most effective algorithm for solution of a given problem. The two-fluid model is the most general model of plasma with local response. In this case, the presented algorithm is probably one of a very few options to solve it. In more simple plasma models, sets of equations with other variables could be more convenient for solution. In the resistive MHD case in addition to variables  $E_{\parallel}, E_{\perp}, v_x$  or  $B_{\parallel}, B_{\perp}, v_x$  (or their analog in other geometries), one can formulate equations in variables  $B_x, j_x, v_x$  and solve them with the Gaussian elimination procedure.<sup>16,17</sup> In the even more simple model of ideal MHD, the most convenient variable seems to be  $v_x$ .

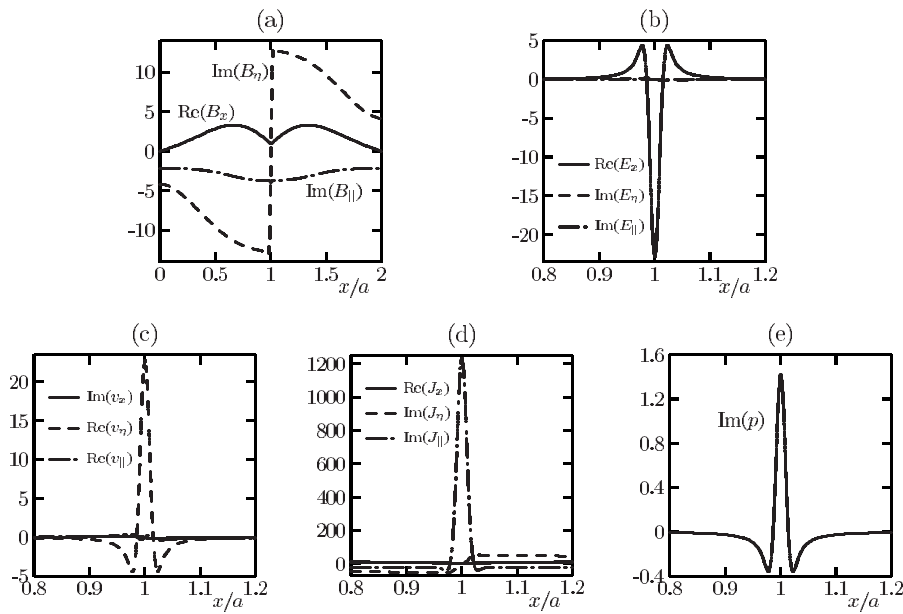


FIG. 2. Field components of tearing mode in resistive MHD model (in arbitrary units).  $\Theta_0=2$ ,  $\alpha_0=2$ ,  $ka=1$ ,  $S=10^5$ ,  $\beta_0=0.3$ .

## V. TEARING EIGENMODES IN THE TWO MODELS

In this section, we present profiles of tearing eigenmodes calculated in the resistive MHD and two-fluid models. Plasma parameters are close to typical parameters in the Madison Symmetric Torus<sup>18</sup> experiment,  $a=50$  cm,  $B_0=1.5$  kG,  $n_e=10^{13}$  cm<sup>-3</sup>; hydrogen plasma is assumed. For these parameters,  $d_i/a=0.14$ ,  $d_e/a=0.0033$ , where  $d_e=c/\omega_{pe}$ . Force-free equilibrium current profile is defined by Eq. (6) with  $\Theta_0=2$ ,  $\alpha_0=2$ . In the calculations, we omit the term  $(\mathbf{v}_e \nabla) \mathbf{v}_e$  in Eq. (12) for simplicity; it does not influence the results for most plasma parameters considered here.

Figure 2 shows profiles of different tearing mode components in the resistive MHD model with  $ka=1$ ,  $S=10^5$ ,  $\beta_0=0.3$ . The growth rate of this mode is  $\gamma\tau_A=0.012$ . Field components are either pure real or pure imaginary; they are normalized such that  $B_x(1)=1$ . Perturbation of magnetic field is

spread over the  $x$  coordinate while the dominant components of electric field and plasma velocity are localized near the resonance surface  $x/a=1$ . We use different scales in  $x$  coordinate for wide and localized functions. Strong perturbation of  $v_\eta$  near the resonance is driven by strong perturbation of  $E_x$  (due to  $\mathbf{E} \times \mathbf{B}$  drift). In spite of a relatively large  $\beta_0$ , the perturbation of  $v_\parallel$  near the resonance is relatively small. This is the effect of plane geometry. In a cylinder, perturbation of  $v_\parallel$  is a dominant component in velocity perturbation for similar plasma parameters. Pressure perturbation is sizable [Fig. 2(e)] meaning that the perturbed plasma flow is compressible.

The components of the two-fluid eigenmode have both real and imaginary parts. They are presented in Figs. 3–5 for the same  $ka$ ,  $S$ , and  $\beta_0$ . The two-fluid growth rate is larger than the resistive MHD one,  $\gamma\tau_A=0.023$ . The same normalization  $B_x(1)=1$  is used. Electron and ion pressure (and den-

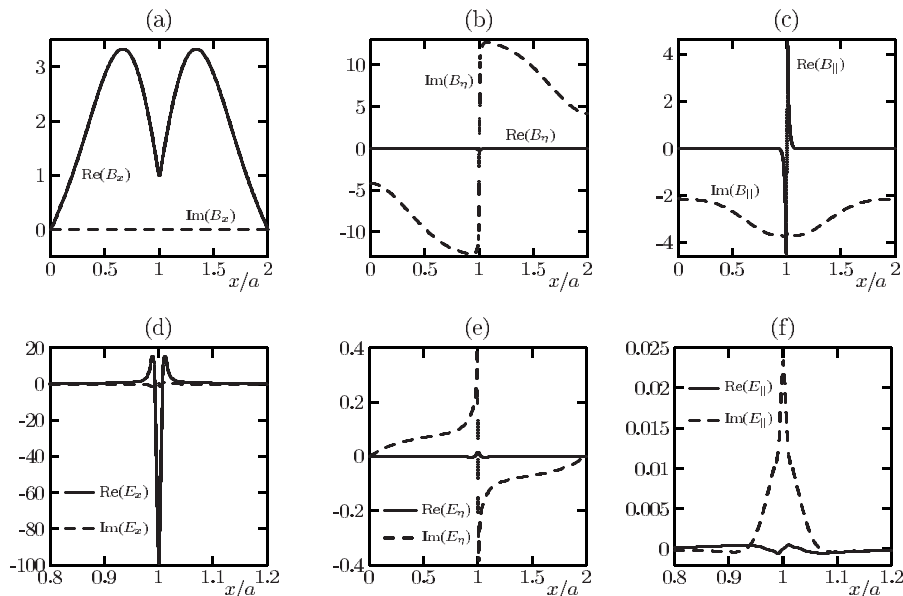


FIG. 3. Field components of tearing mode in two-fluid model (in arbitrary units). (a)–(c) Components of magnetic field. (d)–(f) Components of electric field.  $\Theta_0=2$ ,  $\alpha_0=2$ ,  $ka=1$ ,  $S=10^5$ ,  $\beta_0=0.3$ .

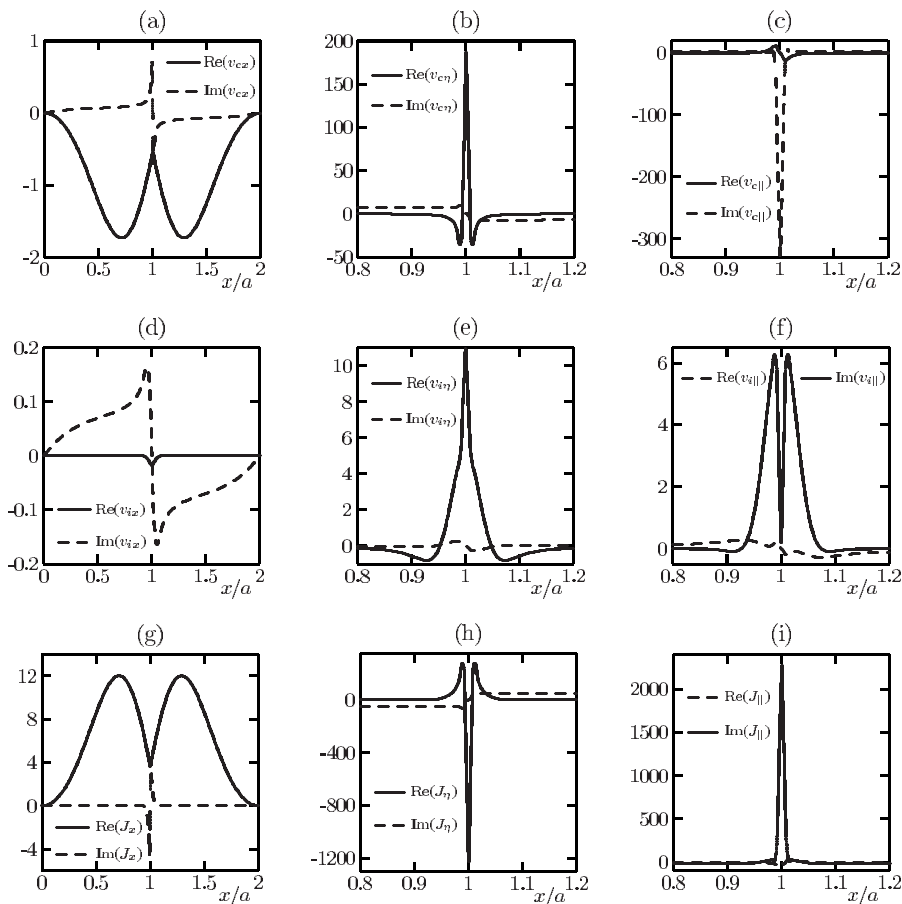


FIG. 4. Field components of tearing mode in two-fluid model (in arbitrary units). (a)–(c) Components of electron velocity. (d)–(f) Components of ion velocity. (g)–(i) Components of plasma current.  $\Theta_0=2$ ,  $\alpha_0=2$ ,  $ka=1$ ,  $S=10^5$ ,  $\beta_0=0.3$ .

sity) perturbations [Figs. 5(a) and 5(b)] are almost identical such that the quasineutrality condition is well satisfied. For these plasma parameters, most of the profiles of the two-fluid eigenmode components are close to the resistive MHD profiles. In the two-fluid case, however, large perpendicular currents appear near resonance surface due to electron-ion decoupling on short scales. These currents drive magnetic field perturbations parallel to the guiding magnetic field, which are localized near the resonance. Also in this geometry in the two-fluid case  $v_{i||}$  is comparable with  $v_{i\eta}$ ; the pressure perturbation is stronger.

For the estimate of the two-fluid effects, we compare different contributions to the generalized Ohm's law. In the normalized variables, the Ohm's law is

$$\begin{aligned} \mathbf{E} + \mathbf{v} \times \mathbf{B} &= \frac{1}{S} \mathbf{j} + \frac{d_i}{a} \frac{1}{n_e} \mathbf{j} \times \mathbf{B} - \frac{\beta_0 d_i}{4} \frac{1}{a n_e} \nabla p_e - \frac{m_e d_i}{m_i a} \frac{d\mathbf{v}_e}{dt} \\ &= \mathbf{R} + \mathbf{H} + \mathbf{P} + \mathbf{I}, \end{aligned} \quad (40)$$

where  $\mathbf{v}$  is the fluid velocity (center-of-mass velocity). The contributions on the right-hand side are identified as the resistive term  $\mathbf{R}$ , the Hall term  $\mathbf{H}$ , the electron pressure gradient term  $\mathbf{P}$ , and the electron inertia term  $\mathbf{I}$ . Components of linearized contributions due to each term near  $x/a=1$  are calculated in Figs. 6(a)–6(c) for the same plasma parameters. We present only dominant contributions that are either purely real or purely imaginary. The result shows that in perpendicular (to local magnetic field) projection of the Ohm's law

(directions  $\mathbf{e}_x$  and  $\mathbf{e}_\eta$ ), the Hall and electron pressure gradient terms dominate. In the parallel projection, resistive and pressure gradient terms dominate with smaller contribution from the electron inertia term while the Hall term is zero. The parallel gradient of plasma pressure drives parallel ion flow near the resonant surface. Thus two-fluid contributions due to Hall and electron pressure gradient terms are sizable for these plasma parameters and they should be accounted for in a more accurate modeling beyond resistive MHD.

We compare the two models by scanning different plasma parameters in Figs. 7(a)–7(c). In all presented cases, the two-fluid growth rate is larger than the growth rate in the

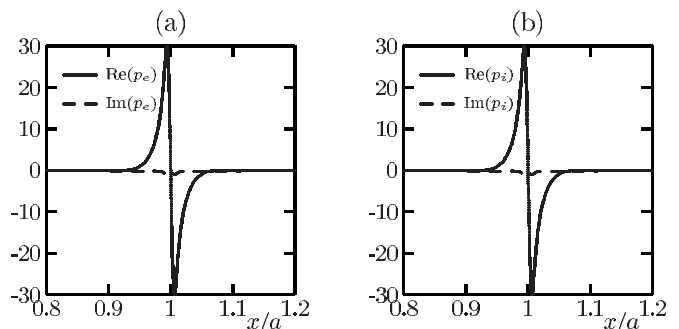


FIG. 5. Field components of tearing mode in two-fluid model (in arbitrary units). (a) Electron pressure; (b) ion pressure.  $\Theta_0=2$ ,  $\alpha_0=2$ ,  $ka=1$ ,  $S=10^5$ ,  $\beta_0=0.3$ .

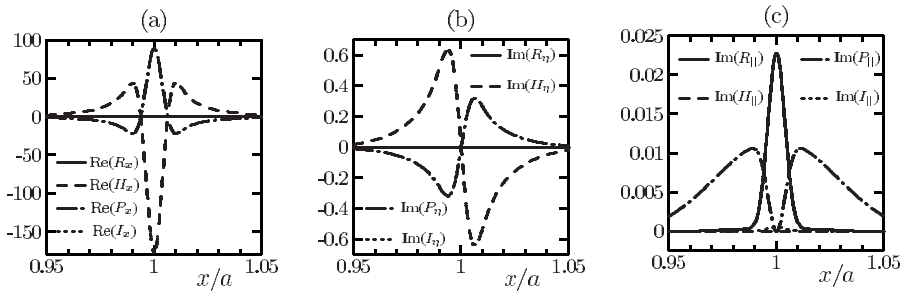


FIG. 6. Contributions to Ohm's law from resistive, Hall, pressure gradient, and electron inertia terms. (a), (b) perpendicular projections; (c) parallel projection.

resistive MHD model for the same plasma parameters. Figure 7(a) shows the dependence of  $\log(\gamma\tau_A)$  versus  $\log S$  (decimal logarithms) for fixed  $ka=1$  and  $\beta_0=0.3$ . At large  $S$ , the scaling of the growth rate in the resistive MHD model is  $\gamma\tau_A \propto S^{-3/5}$ . At higher  $S$ , the two-fluid growth rate will eventually flatten at some value (this range of  $S$  is not presented here) corresponding to the collisionless regime when the electron inertia term is dominant. For the plasma parameters in Fig. 7(a), this transition happens around  $S \sim 10^8$ . The  $\beta_0$  dependence of the growth rate is shown in Fig. 7(b) for  $ka=1$  and  $S=10^5$ . Growth rate is independent of  $\beta_0$  in the resistive MHD model. This is the property of this particular geometry ( $\gamma\tau_A$  reduces with increasing  $\beta_0$  in a cylinder). In the two-fluid model,  $\gamma\tau_A$  increases with the increase of  $\beta_0$  reaching finite limits when  $\beta_0 \rightarrow 0$  and  $\beta_0 \rightarrow \infty$ . The two-fluid growth rate approaches that in the resistive MHD model for smaller  $S$  and  $\beta_0$ . Profiles of  $\gamma\tau_A$  versus  $ka$  for  $S=10^5$  and  $\beta_0=0.3$  are shown in Fig. 7(c). Both resistive MHD and two-fluid growth rates have maxima near  $|ka| \sim 1$ . In both models,  $\gamma\tau_A=0$  for  $ka=0$  and  $\gamma\tau_A \rightarrow 0$  when  $|ka| \rightarrow \infty$ .

## VI. SUMMARY

An algorithm for solving eigenmode problems for resistive MHD and two-fluid plasma equations is formulated. Within each model, a set of equations suitable for numerical solution is derived and the details of the algorithm of this solution are presented. The algorithm is applied for solving for tearing eigenmodes in an RFP-like plasma in plane geometry. The results of resistive MHD and two-fluid models are compared in this case showing that the two-fluid effects on tearing modes in RFPs are sizable. The algorithm is general. It is suitable for solution of boundary (eigenmode) problems for different plasma configurations.

## ACKNOWLEDGMENTS

This work was supported by the U.S. Department of Energy, by the National Science Foundation Center for Magnetic Self-Organization in Laboratory and Astrophysical Plasmas, and by the LDRD program at Los Alamos National Laboratory.

## APPENDIX: OTHER APPLICATIONS OF THE ALGORITHM

We show that the described algorithm is general. It can be applied in different geometries and in different plasma models. We consider two additional examples of application of this approach for finding eigenmodes in cylindrical geometry in resistive MHD model for RFP equilibrium and for radiofrequency waves in the model in which plasma response is defined by a cold plasma dielectric tensor. The latter is related to wave modes in Helicon sources.

We consider a general cylindrical RFP equilibrium with nonuniform current and pressure profiles. Field components are normalized similarly to the slab geometry case. The equilibrium current profile is defined by parameter  $\lambda$  such that

$$\nabla \times \bar{\mathbf{B}} = \lambda \bar{\mathbf{B}} + \mathbf{j}_\perp.$$

$\mathbf{j}_\perp$  is current perpendicular to equilibrium magnetic field; it is related to the pressure gradient. We consider specific profiles

$$\lambda(r) = 2\Theta_0[1 - (r/a)^{\alpha_0}],$$

$$p(r)/p_0 = 1 - 0.99 \exp\left[-\left(\frac{r-a}{0.35a}\right)^2\right]$$

with  $\alpha_0=2$ ,  $\Theta_0=2$ , where  $a$  is the radius of the cylinder. Normalized equilibrium field components satisfy

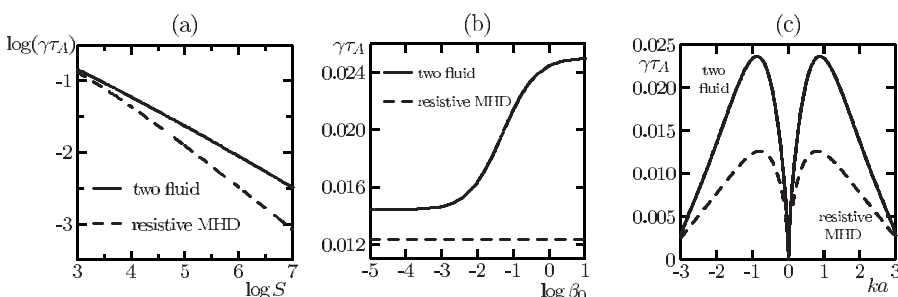


FIG. 7. Comparison of two-fluid and resistive MHD growth rates. (a)  $\log(\gamma\tau_A)$  vs  $\log S$ ; (b)  $\gamma\tau_A$  vs  $\log \beta_0$ ; (c)  $\gamma\tau_A$  vs  $ka$ .

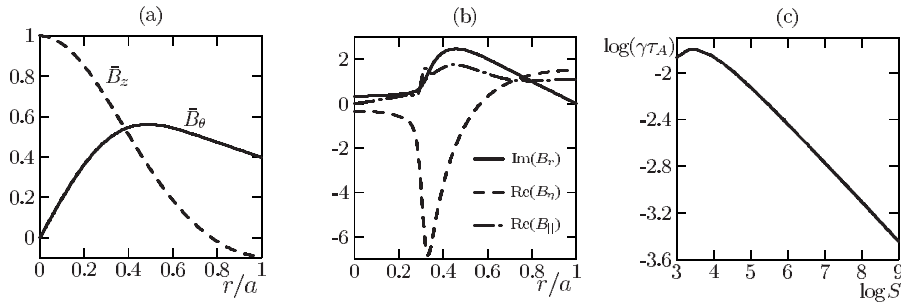


FIG. 8. (a) Equilibrium field components in cylindrical geometry; (b) field components of the eigenmode (in arbitrary units) for  $S=10^5$ ; (c)  $\log(\gamma\tau_A)$  vs  $\log S$ .  $\alpha_0=2$ ,  $\Theta_0=2$ ,  $\beta_0=0.1$ ,  $m=1$ ,  $ka=-2.33$ .

$$\bar{B}'_\theta = -\frac{\bar{B}_\theta}{r} + \lambda\bar{B}_z - \frac{\beta_0\bar{B}_\theta}{2\bar{B}^2}p', \quad \bar{B}'_z = -\lambda\bar{B}_\theta - \frac{\beta_0\bar{B}_z}{2\bar{B}^2}p'$$

with boundary conditions  $\bar{B}_\theta(0)=0$ ,  $\bar{B}_z(0)=1$ . Components of equilibrium magnetic field with these parameters and with  $\beta_0=0.1$  are shown in Fig. 8(a).

Resistive MHD equations in cylindrical coordinates are linearized about this equilibrium and equations for  $B_\eta$ ,  $B_\parallel$ , and  $v_r$  are found in a similar way as in the slab geometry. These equations are Fourier analyzed to find solutions  $\propto \exp(-i\omega t + im\theta + ikz)$ . We consider the core resonant mode with  $m=1$  and  $ka=-2.33$ . The resonance surface of this mode is located at  $r/a=0.3$ . In the considered example, current and pressure gradients are nonzero at the resonance surface. We apply the same algorithm for solving the eigenvalue problem. The difference with the slab geometry is that plasma equations are now in cylindrical coordinates and the boundary conditions at  $r=0$  for the  $m=1$  mode are  $B'_\eta=0$ ,  $B_\parallel=0$ ,  $v'_r=0$ .

Magnetic field components of this mode are presented in Fig. 8(b) for  $S=10^5$ . The dependence of the growth rate versus the Lundquist number  $S$  is shown in Fig. 8(c). At large  $S$ , the growth rate scales as  $S^{-1/3}$ , which is the scaling of the resistive interchange mode.<sup>7</sup> In this example, calculation at large  $S$  is limited by the requirement that the grid size must be small enough to resolve the scale of the most rapidly changing solutions of plasma equations.

In a second example, we consider eigenmodes in cylindrical plasma for radiofrequency waves that are relevant to modes in Helicon sources. Plasma with a nonuniform radial density profile is placed in a uniform axial magnetic field.

We assume that plasma is uniform in poloidal and axial directions and that its response is defined by a cold plasma dielectric tensor<sup>19</sup>

$$\boldsymbol{\epsilon} = \begin{pmatrix} \epsilon_\perp & ig & 0 \\ -ig & \epsilon_\perp & 0 \\ 0 & 0 & \epsilon_\parallel \end{pmatrix},$$

where

$$\epsilon_\perp = 1 - \frac{\omega_{pe}^2}{\omega^2 - \omega_{ce}^2} - \frac{\omega_{pi}^2}{\omega^2 - \omega_{ci}^2},$$

$$g = \frac{\omega_{pe}^2\omega_{ce}}{\omega(\omega^2 - \omega_{ce}^2)} - \frac{\omega_{pi}^2\omega_{ci}}{\omega(\omega^2 - \omega_{ci}^2)},$$

$$\epsilon_\parallel = 1 - \frac{\omega_{pe}^2}{\omega^2} - \frac{\omega_{pi}^2}{\omega^2}.$$

Maxwell's equations

$$\nabla \times \mathbf{E} = i\lambda\mathbf{B}, \quad \nabla \times \mathbf{B} = -i\lambda\boldsymbol{\epsilon}\mathbf{E},$$

where  $\lambda = \omega a/c$  and length is in units of  $a$ , are transformed to cylindrical coordinates and Fourier analyzed. Magnetic field is eliminated from these equations. The resulting equations for components of electric field are

$$\left(\frac{m^2}{r^2} + k^2 - \lambda^2\epsilon_\perp\right)E_r + \frac{im}{r}E'_\theta + i\left(\frac{m}{r^2} - \lambda^2g\right)E_\theta + ikE'_z = 0,$$

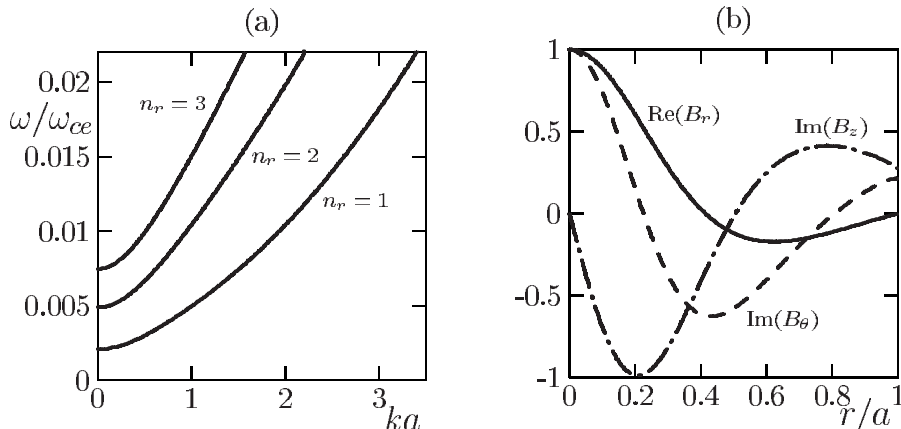


FIG. 9. (a)  $\omega/\omega_{ce}$  vs  $ka$  for first three radial wave numbers; (b) magnetic field components of the eigenmode (in arbitrary units) for  $n_r=2$ ,  $ka=1$ .

$$\left\{ \frac{im}{r^2} \left[ \frac{1}{\varepsilon_{\perp}} (r\varepsilon'_{\perp} + \varepsilon_{\perp} + mg) + 1 \right] - ig\lambda^2 \right\} E_r + E''_{\theta}$$

$$- \frac{1}{r} \left( \frac{mg}{\varepsilon_{\perp}} - 1 \right) E'_{\theta} - \left[ \frac{m}{\varepsilon_{\perp} r^2} (rg' + g + m\varepsilon_{\perp}) + k^2 + \frac{1}{r^2} \right. \\ \left. - \lambda^2 \varepsilon_{\perp} \right] E_{\theta} - \frac{mk}{r} \left( \frac{\varepsilon_{\parallel}}{\varepsilon_{\perp}} - 1 \right) E_z = 0,$$

$$\frac{ik}{r} \left[ \frac{1}{\varepsilon_{\perp}} (r\varepsilon'_{\perp} + \varepsilon_{\perp} + mg) - 1 \right] E_r - \frac{kg}{\varepsilon_{\perp}} E'_{\theta} - \frac{k}{\varepsilon_{\perp} r} (rg' \\ + g) E_{\theta} + E''_z + \frac{1}{r} E'_z - \left( \frac{\varepsilon_{\parallel}}{\varepsilon_{\perp}} k^2 + \frac{m^2}{r^2} - \lambda^2 \varepsilon_{\parallel} \right) E_z = 0.$$

In derivation of these equations, condition  $\nabla \cdot (\boldsymbol{\varepsilon} \mathbf{E}) = 0$  is used to eliminate  $E'_r$  from the equations. This set of equations has a form similar to the equations obtained in Secs. II and III except that velocity does not enter into equations in the cold plasma model. The equations are formulated for variables  $E_{\theta}$  and  $E_z$  for which the boundary conditions at conducting wall,  $E_{\theta}(a) = E_z(a) = 0$ , are specified. These equations are solved by the algorithm discussed in this paper. The matching point is chosen at  $r = a/2$ . There are no resonances in the plasma volume in this case. The grid size in calculations is chosen to be small enough to resolve fast exponentially decaying solutions corresponding to shielding of parallel electric field by electrons with small inertia.

Dispersion curves in the range of operation of Helicon sources for eigenmodes with poloidal wave number  $m=1$  and radial wave numbers  $n_r=1, 2, 3$  are shown in Fig. 9(a) for parameters  $a=15$  cm,  $B_0=1$  kG,  $n_0=10^{12}$  cm $^{-3}$ , and plasma density profile  $n(r)=n_0 \cdot \{\exp[-(r/0.5a)^2] + 1\}/2$ . The upper limit of frequency in this plot corresponds approximately to lower hybrid frequency  $\omega_{LH} = \sqrt{\omega_{ci}\omega_{ce}}$ , where modes with very high radial wave numbers are present,

which complicates calculation of the dispersion curves. Radial profiles of magnetic field components in the eigenmode with  $n_r=2$ ,  $ka=1$ , and  $\omega/\omega_{ce}=0.01$  are shown in Fig. 9(b).

- <sup>1</sup>E. R. Priest and T. G. Forbes, *Magnetic Reconnection: MHD Theory and Applications* (Cambridge University Press, Cambridge, 2000).
- <sup>2</sup>S. Ortolani and D. Schnack, *Magnetohydrodynamics of Plasma Relaxation* (World Scientific, Singapore, 1993).
- <sup>3</sup>D. L. Brower, W. X. Ding, S. D. Terry, J. K. Anderson, T. M. Biewer, B. E. Chapman, D. Craig, C. B. Forest, S. C. Prager, and J. S. Sarff, *Rev. Sci. Instrum.* **74**, 1534 (2003).
- <sup>4</sup>N. Crocker, G. Fiksel, S. C. Prager, and J. S. Sarff, *Phys. Rev. Lett.* **90**, 035003 (2003).
- <sup>5</sup>P. W. Fontana, D. J. Den Hartog, G. Fiksel, and S. C. Prager, *Phys. Rev. Lett.* **85**, 566 (2000).
- <sup>6</sup>W. X. Ding, D. L. Brower, D. Craig, B. H. Deng, G. Fiksel, V. Mirnov, S. C. Prager, J. S. Sarff, and V. Svidzinski, *Phys. Rev. Lett.* **93**, 045002 (2004).
- <sup>7</sup>H. P. Furth, J. Killen, and M. N. Rosenbluth, *Phys. Fluids* **6**, 459 (1963).
- <sup>8</sup>B. Coppi, J. M. Greene, and J. L. Johnson, *Nucl. Fusion* **6**, 101 (1966).
- <sup>9</sup>T. Terasawa, *Geophys. Res. Lett.* **10**, 475, DOI: 10.1029/GL010i006p00475 (1983).
- <sup>10</sup>A. B. Hassam, *Phys. Fluids* **27**, 2877 (1984).
- <sup>11</sup>V. V. Mirnov, C. C. Hegna, and S. C. Prager, *Phys. Plasmas* **11**, 4468 (2004).
- <sup>12</sup>R. Fitzpatrick and F. Porcelli, *Phys. Plasmas* **11**, 4713 (2004).
- <sup>13</sup>N. Bian and G. Vekstein, *Phys. Plasmas* **14**, 072107 (2007).
- <sup>14</sup>J. R. King, C. R. Sovinec, and V. V. Mirnov, *Bull. Am. Phys. Soc.* **52**, 135 (2007).
- <sup>15</sup>S. I. Braginskii, *Reviews of Plasma Physics* (Consultants Bureau, New York, 1965), Vol. 1, p. 205.
- <sup>16</sup>D. H. Liu, J. Li, and T. Hellsten, *Phys. Scr.* **55**, 604 (1997).
- <sup>17</sup>D. H. Liu, *Nucl. Fusion* **37**, 1083 (1997).
- <sup>18</sup>S. C. Prager, J. Adney, A. Almagri, J. Anderson, A. Blair, D. L. Brower, M. Cengher, B. E. Chapman, S. Choi, D. Craig, S. Combs, D. R. Demers, D. J. Den Hartog, B. Deng, W. X. Ding, F. Ebrahimi, D. Ennis, G. Fiksel, R. Fitzpatrick, C. Foust, C. B. Forest, P. Franz, L. Frassinetti, J. Goetz, D. Holly, B. Hudson, M. Kaufman, T. Lovell, L. Marrelli, P. Martin, K. McCollam, V. V. Mirnov, P. Nonn, R. O'Connell, S. Oliva, P. Piovesan, I. Predebon, J. S. Sarff, G. Spizzo, V. Svidzinski, M. Thomas, E. Uchimoto, R. White, and M. Wyman, *Nucl. Fusion* **45**, S276 (2005).
- <sup>19</sup>F. Aleksandrov, L. S. Bogdankevich, and A. A. Rukhadze, *Principles of Plasma Electrodynamics* (Springer-Verlag, New York, 1984).